

RESEARCH ARTICLE

The energy cost of cyclic muscle contractions at different initial muscle-tendon unit lengths derived from near-infrared spectroscopy

Spencer J. Skaper,^{1,2} Jack Z. Jin,¹ Michael J. Asmussen,³ and Jared R. Fletcher¹

¹Department of Health and Physical Education, Mount Royal University, Calgary, Alberta, Canada; ²Department of Medicine, University of British Columbia, Vancouver, British Columbia, Canada; and ³Department of Kinesiology, Vancouver Island University, Nanaimo, British Columbia, Canada

Abstract

During locomotion, the plantarflexor muscle fascicles appear to operate on the ascending limb of its maximal force-length relationship, producing less force per unit activation and elevating the energy cost (EC) compared with contractions performed at optimal length (L_o). The EC of the medial gastrocnemius muscle was quantified at different initial muscle-tendon unit lengths by having participants perform 30 submaximal fixed-end contractions at an ankle joint angle associated with $0.85L_o$, L_o , and $1.15L_o$ in a random order, cyclically targeting 50% of the maximal force at $0.85L_o$. EC was quantified from near-infrared spectroscopy during blood flow occlusion and EMG quantified MG muscle activity. Mean EC was $36 \pm 24\%$ higher at $0.85L_o$ ($P = 0.005$) compared with L_o . Mean EC at $1.15L_o$ ($2 \pm 27\%$ lower) was similar to that at L_o ($P = 0.81$), despite lower forces at $0.85L_o$ ($P = 0.02$), and similar absolute fascicle shortening ($P = 0.10$), and shortening velocity ($P = 0.52$). Muscle activity was approximately twofold higher at $0.85L_o$ ($P = 0.001$). The EC per unit activation was similar across lengths ($P = 0.45$), whereas the EC per unit force was significantly higher at $0.85L_o$ compared with L_o and $1.15L_o$ ($P = 0.008$). Together, these results demonstrate a significant increase in the cost of cyclically producing force at short initial muscle-tendon unit lengths, due to a lower force potential at that initial muscle fascicle length, which we surmise is a result of a lower cross-bridge force and not a higher energetic cost of activation.

NEW & NOTEWORTHY Cyclically producing force performed at short muscle-tendon unit lengths incurs a higher metabolic cost of contraction compared with those contractions performed at optimal or long muscle-tendon unit lengths, respectively. We confirm this through direct observation of muscle fascicle length and muscle energy cost measurements. We further offer a unique and novel explanation for why muscles consume more energy at short compared with optimal or long initial muscle-tendon unit lengths.

energy cost; fascicle length; force-length; near-infrared spectrometry; ultrasound

INTRODUCTION

Lower-leg muscle contractions govern walking and running performance by producing external mechanical work during the stance phase to support and accelerate the body from step to step. The production of external mechanical work during walking and running comes at an energy cost for which the lower-leg muscles are almost exclusively responsible (1). A muscle's energy cost during cyclic contractions is determined by several factors, including, the active rate of muscle fascicle lengthening and shortening, the magnitude of muscle force production (the product of which is muscle fascicle work), the rate of force development, the contraction duration and force-time integral (2, 3), and initial absolute or relative muscle-tendon unit length (4–6). The type of contraction (shortening-only, lengthening then shortening, and isometric) and history-dependent effects might also influence the energy cost of muscle contraction (7, 8). However, the impact of initial muscle-tendon unit length on muscle energy cost, and how initial muscle fascicle

length influences the determining factors of muscle energy cost is not well understood.

For a given (optimal) sarcomere length, a longer muscle fascicle will have more sarcomeres in series, which, when activated, will all produce force and consume metabolic energy proportional to the number of in-series cross bridges that are active (1, 9). Conversely, for a muscle with the same number of in-series sarcomeres, it is not obvious how changes in initial muscle fascicle length (and thus changes in all in-series sarcomere lengths) influences metabolic cost. At shorter than optimal lengths, fewer cross bridges are engaged because of reduced actin-myosin overlap, increased actin-actin overlap of each half sarcomere, or the myosin filament abutting the z-disk at the center of the sarcomere (10). In all cases, force per cross bridge is reduced. To achieve a target force at this shorter than optimal length, additional cross bridges would be required to be active, and with it an elevated cost of activation (11). The same rationale would apply for muscles at longer than optimal length, due to their reduced force potential at longer than optimal



lengths as well. Passive forces at longer than optimal muscle-tendon unit lengths may mitigate the loss of sarcomere force potential due to reduced filament overlap, but this remains to be seen *in vivo*. The notion that initial muscle-tendon unit length influences muscle energy cost during locomotion has largely been ignored (11, 12).

Relative muscle length is typically defined based on some optimal length (L_o) based on the muscle's maximal force-length relationship (10). Across multiple muscle scales, from sarcomeres to whole pennated muscle in series with a compliant tendon [i.e., the muscle-tendon unit (MTU)], short lengths are defined as muscle lengths on the ascending limb of the force-length relationship, or muscle lengths shorter than L_o . Long muscle lengths are considered those on the descending limb, where muscle length is longer than L_o . In both cases, L_o is typically determined from maximally activated muscle contractions. When L_o is determined in this way, the maximal force produced at short and long muscle lengths, respectively, is less than the force produced at L_o . During submaximal cyclic active force contractions, relatively short muscle lengths operating on the ascending limb of the muscle's force-length relationship would necessitate a higher muscle energy cost for at least two main reasons: 1) the level of muscle activation to achieve a given submaximal active force is higher at short lengths due to the reduced force potential at that short length and 2) lattice spacing between actin and myosin increases at short muscle lengths indicating myosin heads are farther from potential binding sites on actin, which alters the direction of active force vectors upon binding (13) resulting in a smaller resultant force vector along the line of muscle shortening; a lower resultant active force per cross bridge would necessitate more active cross bridges to achieve a target force. Therefore, at short muscle lengths, there is less active force per unit activation (14, 15) and adenosine triphosphate (ATP) utilization (16–18). In addition, contractions performed at long initial muscle lengths would also require a higher level of activation to achieve a given submaximal force, because of equally reduced filament overlap but also because actin-myosin lattice spacing is less than optimal, confining the cross bridge heads to a smaller volume and reducing the probability of binding (19). The relative reduction in active force due to lattice spacing is apparently less at long compared with short lengths (13), so the rate of ATP utilization would be reduced at long compared with short muscle lengths, in proportion to the reduced active force potential across muscle lengths.

Higher passive forces, which increase exponentially on the descending limb of the force-length relationship, would also contribute to the total force at long lengths (20), requiring less active force (and thus less metabolic energy) to achieve a target (total) force during cyclic contractions. To further confound the impact of muscle length on metabolic cost *in vivo*, muscles shorten and perform work (21, 22), elevating the metabolic cost to achieve a target force since metabolic cost is proportional to work (22, 23). But passive force is reduced during fascicle shortening (20), and since target (total) force is the sum of active and passive forces, more active force (and higher metabolic cost) would be required to achieve the target (total) force. Finally, lower limb locomotor muscles are often arranged in series with a compliant tendon (24), such that at short MTU lengths, the muscle fascicles are shortened and

the tendon is slack. Additional energy for muscle shortening would be required to take up tendon slack at short muscle-tendon unit lengths. Conversely, at long MTU lengths, in-series tendons are stretched, storing elastic strain energy, which can contribute to total positive mechanical work that would otherwise have to be performed by muscles alone (25). These confounding factors (increased energy cost due to lower active force potential and lattice spacing and passive forces reducing energy cost) have not been explored during cyclic contractions at different initial MTU lengths while calculating active force correctly by appropriately considering changes in passive forces during muscle shortening (20).

The impact of initial muscle length on energy cost is often studied *in vitro* or *in situ* during isometric contractions. In the cases of isometric contractions, initial muscle length is final muscle length, making interpretations of muscle length's impact on energy cost straightforward. However, during *in vivo* locomotion, such as in walking and running, cyclic length changes of muscle fascicles are produced and mechanical work is performed against an in-series tendon. It has long been thought that increased mechanical work alone contributes to increased muscle energy cost. This hypothesis was first proposed by Fenn (23), who first related the magnitude of work done during shortening to the extra energy liberated. This has become known as the Fenn Effect. But contrary to the experiments by Fenn, who altered work by changing the magnitude of force and keeping the shortening fixed, in level-ground walking and running, the average force across strides is constant, and equal to body weight (26). At the muscle fascicle level, force and shortening are varied simultaneously, so work is proportional to active muscle fascicle shortening and lengthening and active force production during each stride. We previously determined that muscle shortening, and not work per se, dictated *in vivo* muscle energy cost (27). In brief, compared with a series of fixed-end plantarflexion contractions where muscle fascicles shorten and perform work to achieve a target force, when additional shortening of the MTU is imposed, muscle fascicle shortening is more, despite participants being unable to achieve the target force. Muscle mechanical work was lower, and muscle energy cost was higher during imposed MTU shortening. We put forth the notion that muscle energy cost was higher during imposed shortening because the velocity of muscle fascicle shortening was higher, necessitating a higher level of activation (and with it a higher metabolic cost of activation) due to the muscle's force-velocity relationship (24, 27). Thus, the suggestion that the energy cost of muscle contraction is proportional to the mechanical work performed is not as straightforward as the Fenn effect would suggest.

Recently, Beck et al. (18) measured whole-body energy cost using indirect calorimetry while performing cyclic fixed-end plantarflexion contractions at apparently short, optimal, and long initial soleus muscle fascicle lengths. These authors found that the energy cost increased by more than twofold at shorter initial muscle fascicle lengths compared with an assumed L_o , defined as an ankle angle of 90°. These authors attributed the elevated energy cost at short initial muscle fascicle lengths to the increased cost of activating more force-producing cross bridges (due to a reduced force per cross bridge) and the accompanying increased cost of muscle activation to achieve a target force. However, inferring muscle energy cost using expired gas analysis assumes that the measured gases at

the mouth accurately reflect those gases at the cellular level of the skeletal muscles (28). This may not be the case for small muscle mass exercise, such as ankle plantarflexion (29). The measured energy cost at the mouth may also reflect the energy cost of other agonist and/or antagonist muscles, accessory muscles that are likely active during the contractions, such as arm, trunk, and abdominal muscles, and the energy cost of supporting cardiac output and ventilation.

To confound these energetic interpretations, the definition of “short” versus “optimal” versus “long” initial and/or final muscle fascicle lengths is almost exclusively based on a maximally activated force-length relationship (18, 30). Assessing final (i.e., shortest) muscle fascicle length using a maximally activated force-length relationship, however, does not consider that muscles are not maximally activated in most locomotor activities. There is an inverse relationship between muscle force and the final muscle length associated with L_o (14, 15, 31) such that L_o is at a longer muscle length at lower force levels and shifts to shorter lengths with increasing muscle force. Indeed, Beck et al. (18) tested the impact of initial muscle fascicle length on metabolic cost at an assumed maximally activated L_o , with the other two lengths on the ascending limb of the (maximal) force-length relationship (see Fig. 2B and Fig. 5D from Ref. 18). As such, longer than optimal muscle fascicle lengths were not evaluated.

To address these concerns, continuous wave near-infrared spectroscopy (NIRS) offers a valid and reliable technique to quantify the muscle-specific energy cost noninvasively (27, 32, 33). The NIRS signal represents a dynamic balance between O_2 supply and O_2 consumption. During occlusion, oxyhemoglobin concentration [O_2Hb], in the absence of inflow and outflow to and from the tissue (i.e., “ O_2 supply”), reflects functional changes induced by local oxidative metabolism and the resynthesis of ATP aerobically (34). Thus, the rate of change of [O_2Hb] represents the rate of muscle oxygen consumption and corresponds to similar values obtained invasively using the direct Fick method (34, 35). Indeed, although the relationship between muscle oxygen uptake using NIRS and whole body oxygen uptake from indirect calorimetry during walking is strong [$r^2 = 0.58$ (36)], whole body oxygen uptake may not reflect the local differences in muscle energy cost that can be detected with NIRS (34).

Quantifying the difference in the energy cost of muscle contractions performed at “short” versus “long” initial MTU lengths have not yet been performed using submaximally determined fascicle force-length relationships, nor has the muscle energy cost been quantified directly. For these reasons, we aimed to quantify the energy cost of muscle contraction at short, optimal, and long MTU lengths using NIRS, based on the muscle’s submaximal force-fascicle length relationship. Therefore, we took the conventional statistical approach to test the null hypothesis that the muscle energy cost of cyclically producing force would be similar across initial muscle fascicle lengths.

METHODS

An a priori sample size was calculated to detect a similar magnitude of difference in muscle energy cost across MTU lengths as reported previously by Beck et al. (18) using indirect calorimetry using G*Power (v. 3.1.9.6). We assumed a Type I

error rate of $\alpha = 0.05$, and statistical power $(1-\beta) = 0.80$. The means \pm SD values for net metabolic power across lengths were extracted from Beck et al. (18) to calculate an appropriate effect size (37) using the web-based program Webplotdigitizer (38). From this computation, we determined that a sample size of $n = 7$ participants was required, and in line with Beck et al.’s sample size ($n = 9$), we recruited an additional two participants for a total sample size of $n = 9$ participants.

Nine participants (6 males, 3 females, 24 ± 3 yr, 68.2 ± 8.1 kg, 172.9 ± 9.6 cm) completed the experimental protocol. For participants to be included in the study, they had to have met the following inclusion criteria: between 18 and 50 yr of age, free of any lower leg muscle or nerve impairment, not currently taking any antihypertensive medication, free of cardiovascular disease, and were normotensive. This study was approved by Mount Royal University’s Human Research Ethics Board (HREB ID No. 102776). All experimental procedures were performed in accordance with the approved protocol and in accordance with the ethical standards of the Declaration of Helsinki. All participants gave informed, written consent to the experimental procedures before participating in the study.

The participants visited the laboratory on a single occasion. Three wireless electromyography (EMG) sensors (Delsys Trigno, Natick, MA) were placed on the right medial gastrocnemius (MG), soleus, and tibialis anterior muscle along the presumed resting pennation angle according to Surface ElectroMyoGraphy for the Non-Invasive Assessment of Muscles (SENIAM) guidelines (39, 40). The resting pennation angle of each muscle was confirmed before sensor placement using ultrasonography. EMG was used to quantify the magnitude of muscle activation, which is the algebraic sum of all single motor unit action potentials activated via a combination of muscle recruitment and rate coding (41). The applied external forces orthogonal to the foot during maximal voluntary contractions (MVCs) were measured using a commercially available instrumented insole (Loadsol, Novel, St. Paul MN), which was affixed to the dynamometer footplate (System 3, Biodex Medical Systems Inc., Shirley, NY). Applied external forces were collected at 100 Hz and were used to calculate the external ankle joint moment (42). External ankle joint plantarflexion moment was calculated from the measured force from the instrumented insole, as described previously by Hullfish and Baxter (42). The instrumented insole comprises three discrete zones modeled as three discrete one-dimensional force plates. The plantarflexion moment is calculated as the scalar product of the measured force applied to each zone and the distance of the center of pressure for each zone to the ankle joint center of rotation. Plantarflexor muscle force was calculated from the previously calculated plantarflexion moment divided by the measured AT moment arm length. Active plantarflexion force was then calculated by considering changes in passive force as a function of MG fascicle length (20). Active plantarflexion force during each MVC at each ankle joint angle was calculated by subtracting the passive force (corresponding to the fascicle length at which peak force occurred) from the total plantarflexion force. The MG force was then scaled from the total plantarflexion active force based on the relative physiological cross-sectional area of the MG to all the plantar flexors (43), then dividing this muscle force by the cosine of the measured pennation angle throughout each contraction (43).

Following this, a B-mode ultrasound transducer [3–4 cm scanning depth, 50 mm field of view, 5–12 MHz (ArtUs, Telemed, Lithuania)] was placed on the right MG muscle belly and secured with tensor bandages. Ultrasound images were collected at 80 Hz during submaximal and maximal plantarflexions and passive cyclical rotations of the right leg. In addition, a NIRS device (PortaMon, Artinis Medical, Zetten, The Netherlands) was placed on the MG belly, distal to the ultrasound probe for measurement of tissue (O_2Hb) desaturation rate during arterial and venous occlusion. Tissue [O_2Hb] was collected at a rate of 10 Hz. A thigh blood pressure cuff was placed proximal to the knee and rapidly inflated before and maintained during each trial to >240 mmHg. Blood flow occlusion was confirmed following each trial by examining the symmetrical change in hemoglobin saturation (decreasing) and desaturation (increasing), suggesting no new arterial blood, and therefore oxygen, had entered the measured region of interest of the muscle during the contractions (44).

Participants laid prone on a fully reclined dynamometer chair with their right knee fully extended (Fig. 1). Their right foot was firmly attached to the dynamometer footplate at 90° (ankle formed by the sole of the foot relative to the long axis of the shank) using a series of Velcro straps. Participants' maximal voluntary ankle range of motion (ROM) was determined by having the participants plantarflex and dorsiflex to their comfort-limited end range of motion. The Achilles tendon (AT) moment arm was estimated using the tendon travel method, accounting for passive forces as described previously by Fletcher and MacIntosh (45). In brief, the ankle was rotated through the range of motion at $0.087 \text{ rad}\cdot\text{s}^{-1}$. During the

rotation, ultrasound images of the MG myotendinous junction were visualized. The translation of the myotendinous junction was considered as the total tendon travel. The AT moment arm was calculated from 85° to 95° (i.e., a rotation of 0.1745 rad) as the ratio of tendon travel (in mm) to joint rotation (in radians). This moment arm was considered the AT moment arm, which we have previously determined is constant throughout the ankle range of motion when plantarflexion passive forces are correctly accounted for (45), which we also confirm here. Participants were then asked to perform maximal voluntary contractions (MVC) at six different ankle joint angles. Ankle joint angles were selected as a fixed percentage of the individual's ankle ROM from 0% (full dorsiflexion) to 100% (full plantar flexion) across 20% ROM intervals. L_f at resting and peak force at each ankle angle were assessed using ultrasonography. During each contraction, muscle force was calculated from the measured ankle joint torque and moment arm lengths. The highest peak force at a given ankle angle was considered maximal force (F_o) for each individual participant. The individual ankle angle at F_o was considered optimal length (L_o) for each participant. Submaximal force versus fascicle-length (mm) relationships were also determined by having participants produce submaximal target forces of 25, 50, and 75% MVC forces (displayed on an external monitor in front of them) at each of the six ankle joint angles (i.e., at 0, 20, 40, 60, 80, and 100% of ankle joint dorsiflexion ROM, where 0% was considered full dorsiflexion). The order of contractions was randomized across joint angles as well as across submaximal force levels. A 2-min rest period was given between contractions to mitigate the effect of muscle fatigue on measured force and/or muscle activation. L_o was considered the ankle angle at which maximum force was produced at each %MVC level.

To assess the impact of MTU length on muscle energy cost, participants performed cyclic contractions at short ($0.85L_o$), optimal (L_o), and long ($1.15L_o$) MTU lengths by altering ankle joint angle before the start of each contractile condition. Participants performed 30 submaximal contractions at 0.5 Hz with a 1-s relaxation period. The frequency of active contraction was controlled by an audible metronome. Target plantarflexion force for each length condition was set at 50% of the maximal plantarflexion force achieved at the short length (i.e., $0.85L_o$) by each participant. The participant-specific target force was displayed on a computer monitor in front of the participants during the trials. After sufficient practice and recovery following practice, participants were asked to reach the target force on the audible tone at the metronome (i.e., at a 0.5-Hz frequency). An exemplar force-time tracing is shown in Fig. 2.

MG muscle EC was assessed using NIRS during blood flow occlusion as described earlier. MG muscle EC was considered as the rate of hemoglobin desaturation during the occlusion trials, calculated as the first derivative of the O_2Hb desaturation signal with respect to time from the 1st to the 10th contraction. For each trial, the rate of O_2Hb desaturation (expressed as $\% \cdot \text{s}^{-1}$) was normalized to the maximal desaturation level of each trial. Immediately following each trial, the thigh blood pressure cuff was released, and a minimum of 5 min was given between trials to ensure adequate lower limb reperfusion. Reperfusion was confirmed before the start of each trial when O_2Hb saturation had returned to baseline.

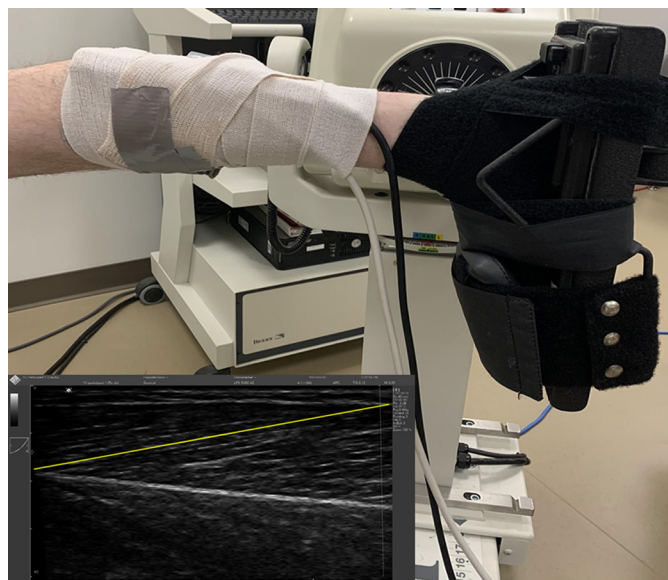


Figure 1. Experimental setup showing a B-mode ultrasound transducer and a NIRS device placed on the MG, distal to the ultrasound probe for measurement of tissue [O_2Hb] desaturation rate during arterial and venous occlusion at a rate of 10 Hz. Both the B-mode transducer and the NIRS device were affixed to the participant's shank using tensor bands and their foot was attached to the dynamometer footplate using Velcro straps. *Inset* shows an exemplar MG ultrasound image, with the yellow line depicting the measured fascicle length at rest. MG, medial gastrocnemius; NIRS, near-infrared spectroscopy; [O_2Hb], oxyhemoglobin saturation.

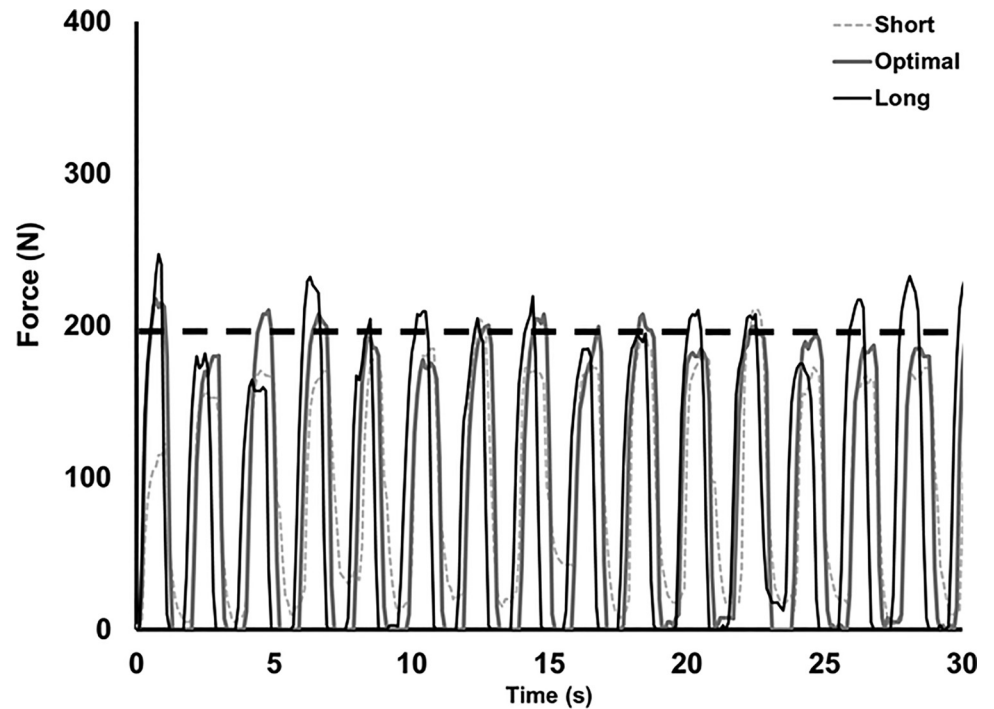
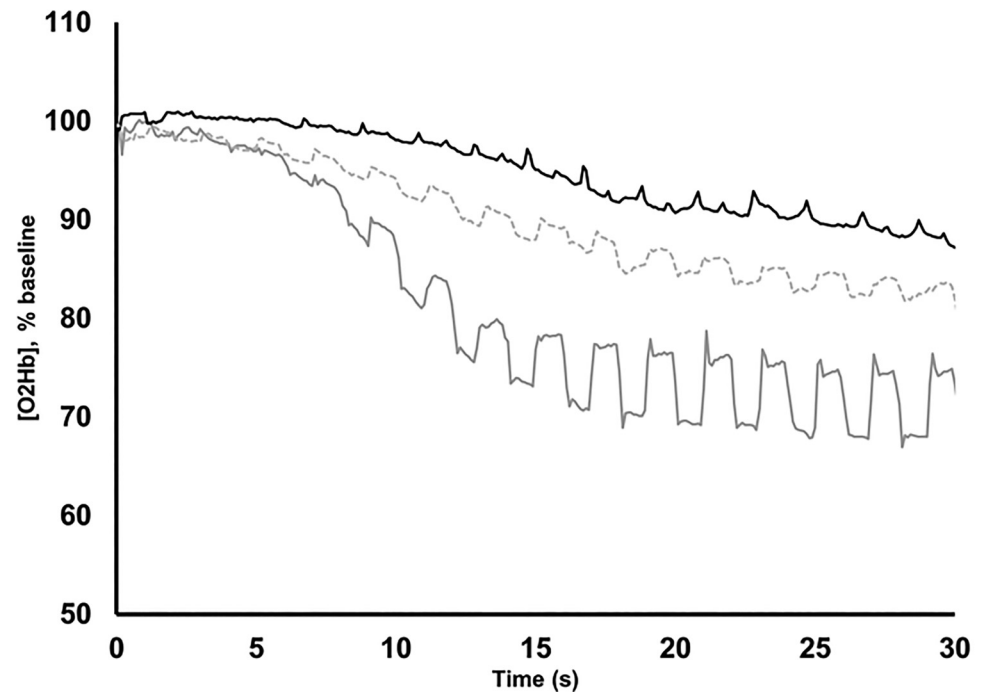


Figure 2. Exemplar force-time and [O₂Hb]-time traces for one participant at short, optimal, and long initial muscle tendon unit lengths. Horizontal dashed line represents target plantarflexor force for that participant. Note: for clarity, only the first 30 s of each condition is shown. [O₂Hb], oxyhemoglobin saturation.



Data Analysis

MG muscle activation during the maximal and submaximal force-length trials as well as in all three blood occlusion trials was quantified from the fourth order band-pass-filtered raw muscle EMG signals between 20 and 450 Hz. The magnitude of muscle activation was quantified as the root mean square of the rectified EMG signals using a 40-ms moving window (20-ms overlap). The average RMS across all cyclic

contractions was considered the level of muscle activation for each muscle length.

B-mode ultrasound images were recorded throughout each trial to determine MG fascicle length change (L_f). L_f during each occlusion trial was measured manually using a publicly available image analysis software (ImageJ, NIH, Baltimore, MD). Shortening velocity (V) was expressed relative to maximal shortening velocity (V_{max}), from the measured fascicle shortening velocity (expressed in $L_f \cdot s^{-1}$) and assuming a V_{max}

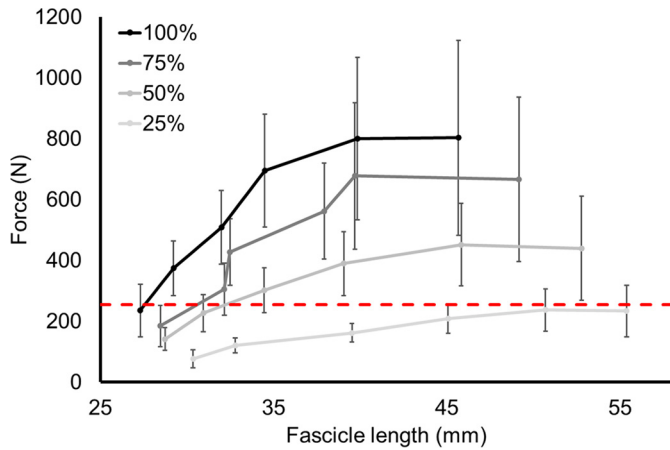


Figure 3. MG force-fascicle length relationship at 25, 50, 75, and 100% maximal force. Mean fascicle length at L_o at 100% MVC was 40.3 ± 11.8 mm, whereas mean fascicle length at 25% MVC was 53.8 ± 9.6 mm. Mean optimal fascicle length increased linearly ($r^2 = 0.999$, $P < 0.0001$) with reduced %MVC ($P < 0.001$ for main effect of %MVC). A horizontal dashed line represents the target force during occlusion trials at short, optimal, and long L_f . Data are presented as means \pm SD for $n = 9$ participants (6 males, 3 females). L_f , fascicle length; L_o , optimal length; MG, medial gastrocnemius; MVC, maximal voluntary contraction.

of the medial gastrocnemius of $10.6 L_f s^{-1}$. This V_{max} was calculated as an average for the entire MG muscle, assuming that the maximal shortening velocity of Type I and Type II muscle fibers were 4.4 and $16.8 L_f s^{-1}$ at physiological temperatures, respectively (12), and assuming that the MG comprised 50% Type I fibers (46). The MG fascicle operating range on the fascicle force-velocity relationship, scaled to activation (47), was then estimated from the calculated fascicle shortening velocity and the computed fascicle force, scaled to maximal isometric force. The latter was considered as the maximal isometric plantarflexion force at L_o .

At each MTU length, the rate of force development (RFD), impulse, and muscle fascicle work were calculated for each contraction. RFD ($N \cdot s^{-1}$) was calculated from the start of each cyclic contraction to the peak force of each contraction. Force impulse (Ns) was calculated as the integral of fascicle force over time throughout the trials and positive MG fascicle work was calculated as the integral of fascicle force and fascicle shortening throughout the trials from rest. The energy cost per unit force was calculated as the ratio of average muscle EC to average MG force during each trial. The energy cost per

unit activation was calculated as the ratio of average MG EC to the average MG EMG root mean square during each trial.

Statistics

Values are presented as means \pm SD. Statistical analysis was performed using JASP (Ver. 0.16.2.0, Amsterdam, The Netherlands). A one-way repeated measures ANOVA was used to test for any potential differences in the measured variables across muscle lengths (where a significant main effect of length was found, Holm’s post hoc tests were used to determine specific differences between muscle lengths). Shapiro–Wilk tests were performed to test for the normality of all dependent variables and where assumed sphericity was violated, a Greenhouse–Geisser corrected P value is reported. The a priori level of statistical significance was set at $P < 0.05$.

RESULTS

Force-Fascicle Length Relationship

The maximal and submaximal force-fascicle length relationships are shown in Fig. 3. Mean fascicle length at L_o at 100% MVC was 40.3 ± 11.8 mm. A significant main effect of % MVC was seen such that optimal fascicle length increased linearly ($r^2 = 0.999$, $P < 0.0001$) with reduced %MVC ($P < 0.001$ for main effect of %MVC).

Muscle Fascicle Dynamics

Muscle fascicle force and length changes measured during each trial are shown in Table 1. A significant main effect of resting L_f across trials was seen ($P < 0.001$). Resting L_f at $0.85L_o$ was significantly shorter, and L_f at $1.15L_o$ was significantly longer than L_f at L_o , respectively ($P < 0.001$).

During cyclic contractions, peak MG muscle force was not significantly different across length conditions ($P = 0.10$) and contraction frequency was also not significantly different across lengths ($P = 0.22$), suggesting participants were able to match target force across length conditions. Force impulse was thus not significantly different across lengths ($P = 0.553$).

Owing to the reduced maximal force potential at short lengths, the target force was $54 \pm 6\%$ of maximum force potential at $0.85L_o$. This relative force was significantly greater than the relative force at L_o ($28 \pm 7\%$, $P < 0.001$) or $1.15L_o$ ($30 \pm 11\%$, $P < 0.001$), respectively. At target force, a significant main

Table 1. Calculated muscle mechanical variables across MG lengths

Variable	Short	Optimal	Long	Main Effect of Length
				P Value
MG muscle force, N/contraction	1,230 \pm 433	1,308 \pm 396	1,353 \pm 462	0.103
Resting fascicle length, mm	45.3 \pm 5.5	59.6 \pm 6.7	63.8 \pm 5.6	<0.001
Fascicle length at target force, mm	31.2 \pm 6.6	47.8 \pm 7.5	53.6 \pm 7.0	<0.001
Fascicle shortening velocity, mm/s	13.3 \pm 7.3	10.5 \pm 4.6	10.7 \pm 8.1	0.517
$L_f s^{-1}$	0.29 \pm 0.15	0.17 \pm 0.08	0.17 \pm 0.13	0.024
V/V_{max}	0.027 \pm 0.014	0.016 \pm 0.007	0.016 \pm 0.012	0.024
Cycle rate, Hz	0.50 \pm 0.03	0.50 \pm 0.03	0.49 \pm 0.02	0.222
Impulse, Ns/contraction	1,231 \pm 423	1,288 \pm 511	1,229 \pm 387	0.553
Mechanical work, J/contraction	17.7 \pm 9.5	15.2 \pm 6.3	14.0 \pm 7.8	0.386

Values are means \pm SD. L_f , fascicle length; MG, medial gastrocnemius; V/V_{max} , muscle shortening velocity relative to maximum shortening velocity. Significant main effects of length ($P < 0.05$) are emphasized in bold.

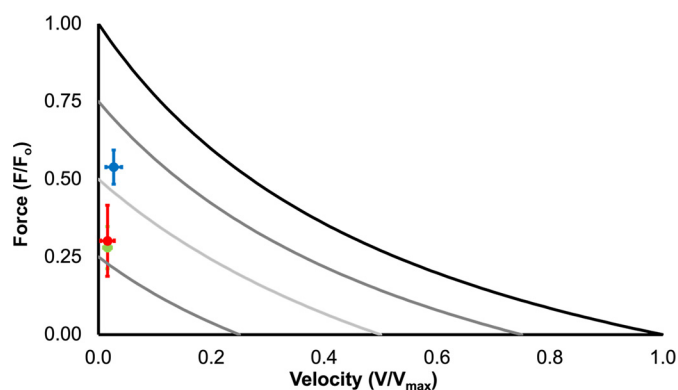
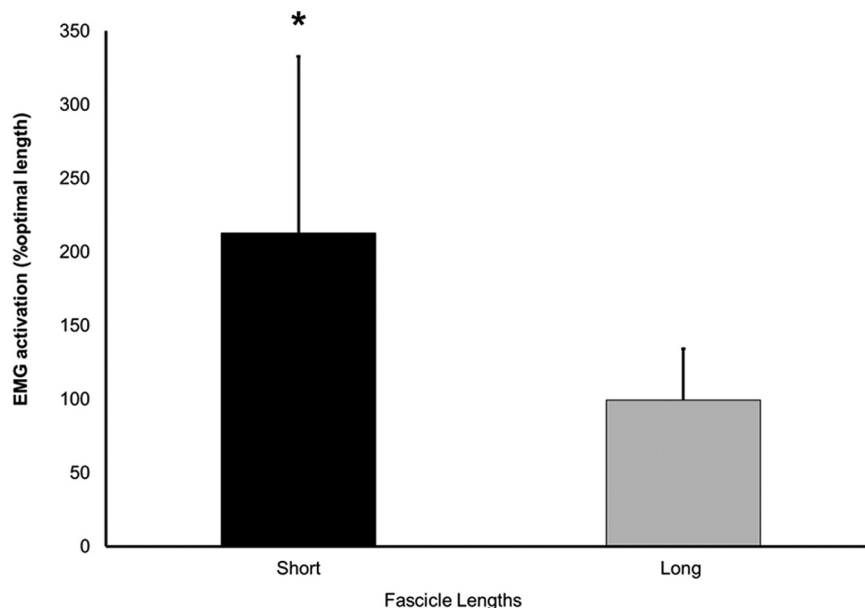


Figure 4. MG force-velocity relationship. The predicted operating range of the MG muscle fascicles on its maximal force-velocity relationship (shown in black) and scaled to 25, 50, and 75% activation (gray lines) (47). Muscle operating range at short (blue), optimal (green), and long (red) lengths, respectively. Expressed relative to initial L_f , shortening velocity is shown to be significantly greater at short, compared with either optimal or long ($P = 0.04$) initial muscle-tendon unit lengths. Data are presented as means \pm SD for $n = 9$ participants (6 males, 3 females). F/F_o , active force relative to maximum; L_f , fascicle length; MG, medial gastrocnemius; V/V_{max} , muscle shortening velocity relative to maximum shortening velocity.

effect of length was seen for L_f such that L_f was shortest at $0.85L_o$ and longest at $1.15L_o$ ($P < 0.001$). Expectedly, L_f at target force was significantly shorter at $0.85L_o$ ($P < 0.001$) and significantly longer at $1.15L_o$ ($P = 0.006$) compared with the mean L_f at L_o . Taken together, the amount of fascicle shortening was not significantly different across lengths ($P = 0.10$). Mean fascicle shortening during each trial was 14.1 ± 4.6 mm, 11.8 ± 4.1 , and 10.2 ± 4.6 mm for $0.85L_o$, L_o , and $1.15L_o$, respectively. Positive muscle mechanical work was also not significantly different across trials ($P = 0.386$).

Fascicle shortening velocity (absolute, in $\text{mm} \cdot \text{s}^{-1}$) was not significantly different across lengths ($P = 0.517$); however, when expressed relative to resting L_f , shortening velocity (in $L_f \cdot \text{s}^{-1}$) was significantly greater at short, compared with either optimal or long lengths ($P = 0.04$). From force and velocity, the predicted operating range of the MG muscle fascicles on its force-velocity relationship is shown in Fig. 4. The average

Figure 5. Average MG muscle activation during cyclic contractions at short and long muscle lengths. Data are expressed relative to activation at optimal length. Short MG L_f was significantly higher than either optimal or long ($P = 0.003$). Muscle activation at long MG L_f ($99 \pm 33\%$ of optimal) was not significantly different than the activation at optimal L_f ($P = 0.983$). *Significantly different, short vs. other lengths. Data are presented as means \pm SD for $n = 9$ participants (6 males, 3 females). For clarity, muscle activation at optimal length is expressed as 100%. EMG, electromyography; L_f , fascicle length; MG, medial gastrocnemius.



force relative to maximum force (F/F_o) and average velocity relative to maximum shortening velocity (V/V_{max}) were both significantly greater at $0.85L_o$ compared with either L_o , or $1.15L_o$ ($P < 0.001$ for force and $P = 0.024$ for velocity, respectively). The estimated level of activation ($58 \pm 19\%$) to achieve target force at this shortening velocity was significantly greater at $0.85L_o$ compared with either L_o or $1.15L_o$ ($28 \pm 9\%$, $P < 0.001$). Indeed, the measured level of MG muscle activation, shown in Fig. 5, was $212 \pm 105\%$ greater at $0.85L_o$ compared with L_o ($P = 0.003$). MG activation at $1.15L_o$ ($99 \pm 33\%$ of optimal) was not significantly different than that measured at L_o ($P = 0.983$), consistent with the activation level required to generate the target force shown in Fig. 3.

Muscle Energetics

NIRS-derived muscle EC relative to L_o is shown in Fig. 6. NIRS-derived muscle energy cost at $0.85L_o$ was $36.4 \pm 24.2\%$ greater than L_o ($P = 0.003$). Muscle energy cost at $1.15L_o$ was similar to that measured at L_o ($-2.4 \pm 27.7\%$, $P = 0.808$). The energy cost per unit activation and the energy cost per unit force are shown in Fig. 7. No significant main effect of MTU length on energy cost per unit activation was seen ($P = 0.45$). However, a main effect of MTU length on the EC per unit force was demonstrated ($P = 0.03$); the EC per unit force was significantly higher at $0.85L_o$ compared with either L_o and $1.15L_o$ ($P = 0.03$ and $P = 0.01$, respectively). EC per unit force was similar between L_o and $1.15L_o$ ($P = 0.47$).

DISCUSSION

In the present study, the EC of submaximal cyclic contractions at short MTU lengths was higher compared with optimal or long MTU lengths. The increased EC at short lengths can be attributed to a twofold increase in muscle activation and a lower economy of force generation at short muscle fascicle lengths. Increased muscle activation in short MG fascicle lengths is largely attributed to a greater relative force in addition to an elevated relative shortening velocity at short lengths. A higher relative force at short lengths is likely due to

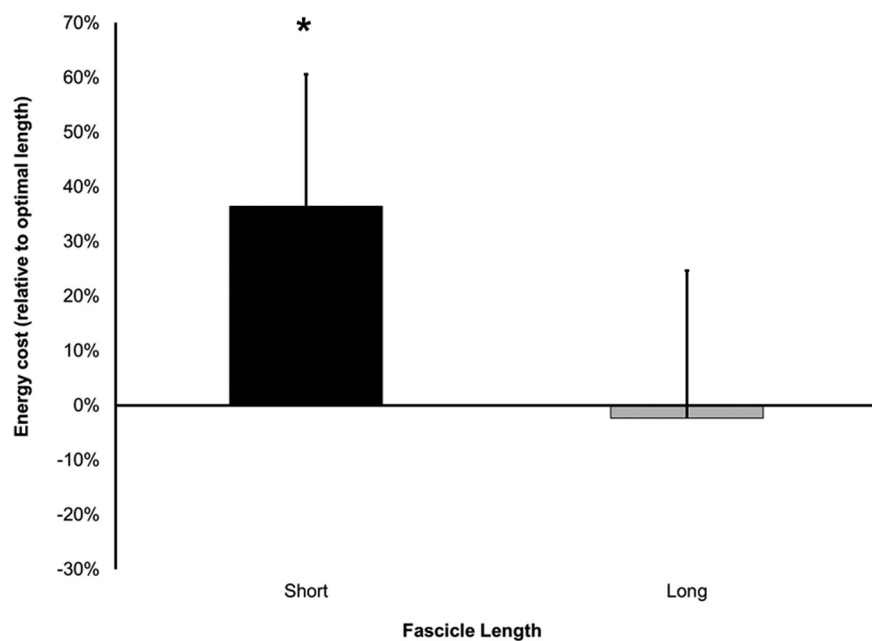


Figure 6. Muscle energy cost of performing submaximal cyclic contractions at short and long fascicle lengths. Data are presented as means ± SD for $n = 9$ participants (6 males, 3 females), and are expressed relative to the energy cost at optimal length. Muscle energy cost of short lengths was $36.4 \pm 24.2\%$ greater than optimal ($P = 0.003$). Muscle energy cost at long was similar ($-2.4 \pm 27.7\%$, $P = 0.808$) to the energy cost at optimal. *Significantly different, short vs. other lengths.

less myofibril overlap, increased actin-actin overlap of each half sarcomere, or the myosin filament abutting the Z-disk at the center of the sarcomere (10) relative to optimal or long lengths, and a greater lattice spacing between actin and myosin filaments. Our findings are consistent with the study by Gordon et al. (10), which showed that relatively short sarcomere lengths result in less overlap between actin and myosin filaments, thus decreasing the muscle’s maximum force potential. Indeed, as evidence from the target force being produced on the steep ascending limb of the MG force-length relationship (see Fig. 2), we cannot discount either actin-actin overlap or the myosin filament abutting the z-disk at these short lengths. Subsequently, relatively short muscle fascicle lengths require greater muscle activation to produce a given submaximal force, which in turn increases EC.

We also show here that initial MTU length affects the relative muscle shortening velocity, since greater shortening is

required to achieve a (higher) relative force at short MTU lengths. Additional fascicle shortening would also be required to take up greater tendon slack at short MTU lengths. Since these submaximal contractions were constrained to be performed at the same cycle frequency (i.e., 0.5 Hz), additional (but nonsignificant) fascicle shortening at short MTU lengths resulted in greater relative fascicle shortening velocities. As shown in Fig. 4, both the higher relative force and the higher relative shortening velocity would elevate the level of muscle activation, and the EC of activation, the associated cost of active ion pumping, $\text{Na}^+ - \text{K}^+$ ATPase, and the sarcoendoplasmic reticulum Ca^{2+} ATPase (SERCA) pumps (48). In addition, our results are in line with those of Hibler et al. (16) who demonstrated a lower force economy of rabbit psoas muscle at short muscle lengths (i.e., 80 and 60% of optimal) compared with optimal length. Together, these findings suggest that sarcomere force production decreases faster than the decrease in ATP utilization at short muscle lengths because an increased lattice spacing between myofibrils alters the cross-bridge force vector upon binding (13). Therefore, at short muscle lengths, there is less cross-bridge force per unit activation as a result of both muscle length and relative muscle shortening velocity. Together, energy cost is elevated at short lengths due to a lower force economy, resulting in less force per unit activation, without a change in the energetic cost per unit activation, in addition to a reduced force potential at short lengths, and a higher level of activation to achieve a given submaximal force. Because positive mechanical work performed by the MG was also not different between conditions, a higher EC at short MTU lengths would also imply a lower muscle efficiency at short lengths, an additional detail that is not considered in many muscle energetic models (49, 50). Together, we have summarized the primary mechanisms of an elevated cost of cyclic muscle contractions that, we believe, are influenced by initial MTU length in Fig. 8.

Beck et al. (18) inferred muscle energy cost from the measured whole body net energy cost via indirect calorimetry, showing a 200% increase in the net EC of cyclic contractions

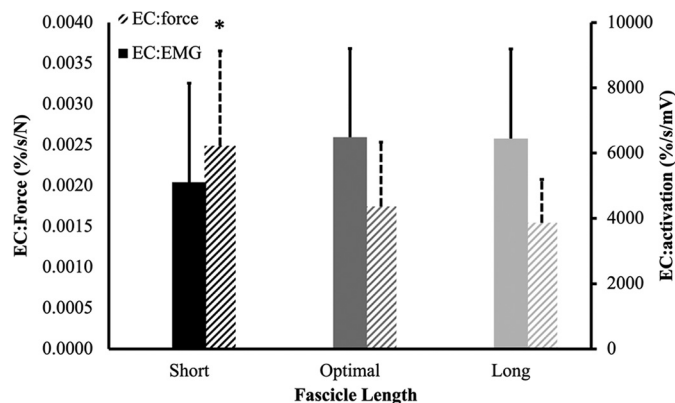


Figure 7. Energy cost per unit activation (solid bars) and energy cost per unit force (hashed bars) across muscle lengths. Energy cost per unit activation was similar across lengths ($P = 0.45$); however, the energy cost per unit force was significantly higher at short compared with optimal and long lengths ($P = 0.03$ and $P = 0.01$, respectively). Data are presented as means ± SD for $n = 9$ participants (6 males, 3 females). *Significantly different, short vs. other lengths. EC, energy cost; EMG, electromyograph.

at short muscle lengths compared with optimal lengths. These measurements may be an overestimate of the muscle-specific energy cost, as it likely included the energy cost of other agonist and antagonist muscles due to changes in the task requirements. To better infer the MG-specific EC across muscle lengths, we used NIRS during arterial occlusion, which offers a valid and reliable technique to isolate and quantify the muscle-specific EC noninvasively and without discomfort (27, 32, 33) and corresponds to similar values obtained invasively using the direct Fick method (52). Using NIRS, we show that at short MG muscle fascicle lengths, the EC increased by 36 and 39% in comparison with optimal and long fascicle lengths, respectively, which are lower than those previously reported by Beck et al. (18). This discrepancy may be due to indirect calorimetry including whole body metabolic costs, whereas a NIRS device allows for the isolation of muscle-specific oxygen consumption based on the site of probe placement (27, 32, 33). Together though, our results are consistent with those of Beck et al. (18) in demonstrating that cyclic contractions performed at short initial MTU lengths increase muscle and whole body energy cost in vivo.

Contributions to the increased EC include increased lattice spacing at relatively short L_f alters crossbridge-crossbridge

geometry and kinetics and decreases force-producing filaments and force per ATP utilization. These changes require the activation of more force-producing cross bridges and the associated cost of active ion pumping, $\text{Na}^+ - \text{K}^+$ ATPase, and the sarcoendoplasmic reticulum Ca^{2+} ATPase (SERCA) pumps (48). During an isometric contraction, the energy cost of ion pumping accounts for 30%–40% of the total EC, with the remaining cost associated with cross-bridge cycling (53, 54). When shortening occurs, the relative proportion of ion pumping is less because shortening considerably increases the cross-bridge turnover (55). During fixed-end contractions performed in vivo, such as seen here, the EC is elevated considerably compared with isometric contractions because the muscle must shorten against the series elastic element (i.e., the tendon). At short muscle fascicle lengths, muscles must shorten more to take up additional in-series compliance, elevating the energy cost of contraction (24, 27).

Many of the previous muscle energetic models have directly or indirectly neglected to consider the impact of initial MTU length on the energy cost of cyclic force contractions. Specifically, some energetic models fail to consider the length-dependent activation of the force-length relationship (14, 56). Although not a model, Beck et al. (18) reported a

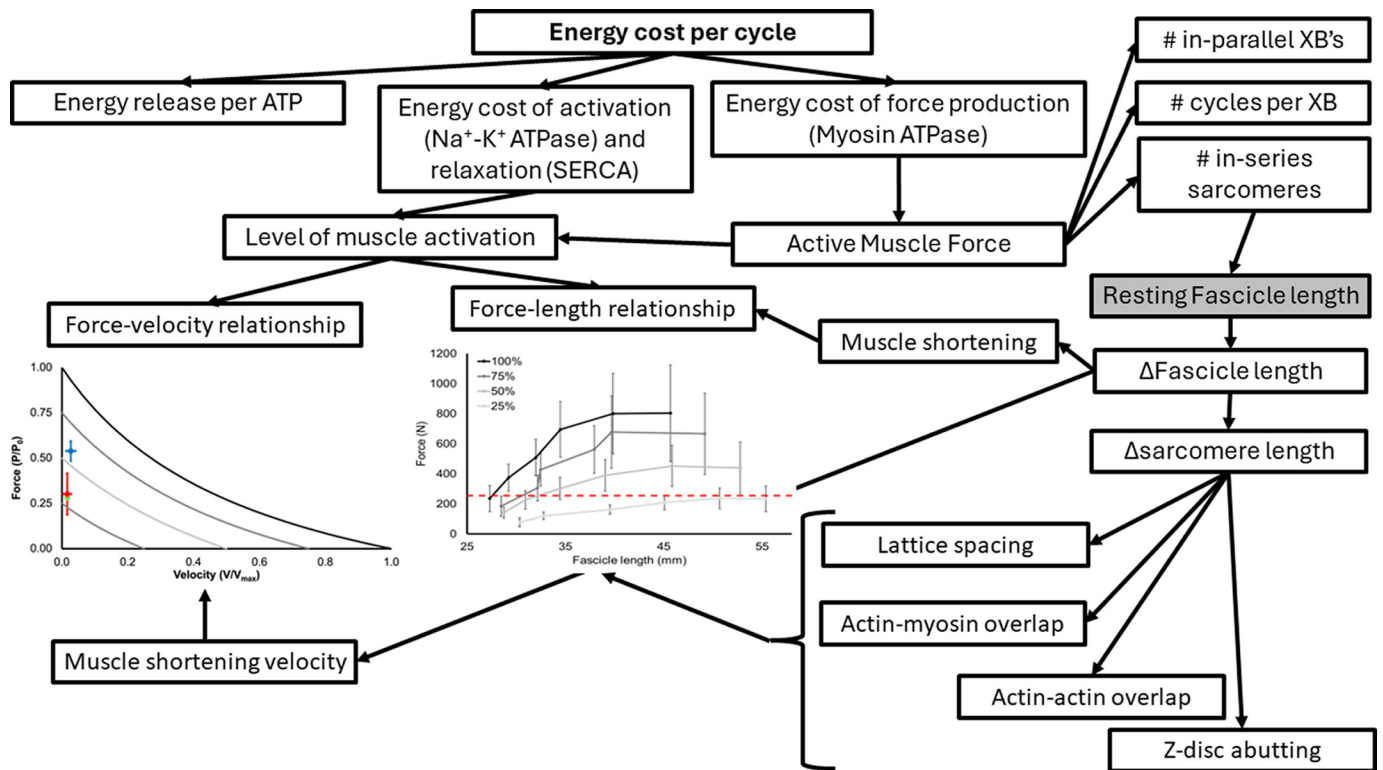


Figure 8. Conceptual framework from a muscle energetics perspective how initial resting muscle fascicle length may influence the energy cost of cyclic force production in vivo. The energy cost per cycle is influenced by the energy cost of activation (associated with ion pumping), and the cost of force production. We have assumed that the energy release per ATP is constant in this framework. To achieve a target active muscle force, muscles must be activated (consuming metabolic energy), the level of which is dictated by the muscle’s force-length and force-velocity relationships. The energy cost of active force production is dictated by the number if parallel and in-series sarcomeres and the number of cycles per cross bridge to sustain or develop the force (for review, see Refs. 1 and 51). Resting fascicle length together and independently alters the change in fascicle length during contraction, which is reflected in a concomitant change in sarcomere length. At short lengths, force potential is reduced due to contractile protein (actin and myosin) overlap and abutting of the z-disk, reducing the number of available cross bridges to produce force. Lattice spacing is also impacted by shortening because of the isovolumetric nature of the muscle fiber. Together, force is reduced and greater activation is required to achieve the target active muscle force. ATP, adenosine triphosphate; $\text{Na}^+ - \text{K}^+$ ATPase, sodium-potassium ATPase activity; SERCA, sarcoendoplasmic calcium ATPase activity; XB, cross bridge.

146%–196% increase in MG muscle activation at short lengths, likely a contributing factor for their reported 200% increased muscle EC. However, Beck et al. (18) assumed all active soleus muscle fascicles had the same maximum shortening velocity and an assumed L_0 to be at an ankle joint angle of 90° . In the current study, MG optimal length was experimentally determined for each participant to be 20% of maximal dorsiflexion angle, which corresponds to an L_0 at an ankle angle of $89 \pm 3^\circ$, like that assumed by Beck et al. (18). Furthermore, relatively short MG fascicle lengths increased EC largely due to a twofold increase in muscle activation and reduced force economy. Medial gastrocnemius muscle fascicles F/F_0 increased due to the altered fascicle geometry (increased lattice spacing), affecting the myosin head's ability to bind with binding sites on actin and altering force vectors upon binding such that the cross-bridge force vector may not be directed parallel to the sarcomere shortening (13). Therefore, short muscle lengths produce less force per unit activation (10, 57), and adenosine triphosphate (ATP) utilization would increase (16–18).

In addition, at $0.85L_0$, relative shortening velocity was increased because fascicles contract over a greater shortening distance in the same period of time against the series elastic element compared with the other longer MTU lengths to achieve the same absolute target force. At short lengths, not only is the force potential reduced, necessitating more engaged cross bridges, but they also must shorten against a relatively slack in-series tendon. Thus, altering initial muscle fascicle length elevates the metabolic cost at short lengths due to both force-length and force-velocity considerations. At $0.85L_0$, the target force represented a higher relative force [50% of maximum force potential (F_0) compared with either L_0 or $1.15L_0$, which were both $\sim 25\%$ of F_0]. Together, the increased F/F_0 , V/V_{\max} , and lattice spacing at short muscle fascicle lengths all contribute to increased muscle activation to achieve the target force at short lengths, elevating the metabolic cost. These findings are in line with those previously shown by Beck et al. (18), who demonstrated an $\sim 200\%$ increase in soleus and lateral gastrocnemius activation with increasing ankle angle (and thus increasing plantar-flexor muscle length).

In the present study, we acknowledge that we did not explicitly control for various factors associated with the cyclic muscle contractions. These factors include the force-time integral (i.e., impulse), muscle shortening velocity, and muscle mechanical work. However, each of these factors showed no significant differences across length conditions, although a moderate effect for absolute fascicle shortening was seen at short versus optimal and long lengths, respectively. To better understand the impact of muscle fascicle shortening velocity on muscle EC, isokinetic concentric and eccentric contractions should be performed to better predict muscle EC during locomotion. Our muscle activation was estimated from a surface EMG signal. Given that the EMG signal can be distorted due to amplitude cancellation, changes in electrode position during a contraction, signal source changes from muscle length changes, and cross talk, the activation measure may not be an exact replicate of true muscle activation. This difference, as a result, could influence our modeled muscle energy cost. We also acknowledge

both the region-specific muscle energy cost and MG fascicle length measures of the NIRS and ultrasound imaging, which may not be reflective of the whole MG muscle, and certainly not necessarily be indicative of the whole triceps surae muscle groups energetics and mechanics at different MTU lengths. Furthermore, future studies should investigate the effects of the stretch-shortening cycle contractions (i.e., shortening and lengthening of the muscle and/or muscle-tendon unit) to better elucidate mechanisms of altered muscle and whole body energy cost across a wide variety of locomotor conditions where muscle length may be altered.

Conclusions

In conclusion, the present study showed that muscle energy cost of submaximal cyclic contractions performed at a short initial muscle-tendon unit length was 36.4% higher than the energy cost of performing the same cyclic contractions at optimal or longer muscle-tendon unit lengths. The elevated muscle EC at short muscle-tendon unit lengths can be attributed to an increased muscle activation due to reduced force potential and a lower force per cross bridge at short muscle fascicle lengths. The latter mechanism has been proposed to elevate muscle energy cost at short muscle lengths due to greater lattice spacing between myofilaments as well as a reduced force per cross bridge with an elevated muscle shortening velocity. These data contribute to a fundamental understanding of how muscles' force-length-velocity relationships together and independent of a muscle in series with a compliant tendon affect the energy cost of muscle contraction in vivo and highlight the importance of considering the (submaximal) force-length and force-velocity relationships of in vivo skeletal muscle together, and not alone.

DATA AVAILABILITY

The datasets generated during and/or analyzed during the current study are available from the corresponding author on reasonable request.

ACKNOWLEDGMENTS

The authors thank Haleigh Mills and Talia Piperni for assistance with data collection.

GRANTS

This study was supported by the Natural Sciences and Engineering Research Council (NSERC) of Canada (Grant No. RGPIN-2020-04817).

DISCLOSURES

No conflicts of interest, financial or otherwise, are declared by the authors.

AUTHOR CONTRIBUTIONS

J.R.F. conceived and designed research; S.J.S., J.Z.J., and J.R.F. performed experiments; S.J.S., J.Z.J., and J.R.F. analyzed data; S.J.S., M.J.A., and J.R.F. interpreted results of experiments; J.Z.J. and J.R.F. prepared figures; S.J.S. and J.R.F. drafted

manuscript; S.J.S., J.Z.J., M.J.A., and J.R.F. edited and revised manuscript; S.J.S., J.Z.J., M.J.A., and J.R.F. approved final version of manuscript.

REFERENCES

1. **Fletcher JR, MacIntosh BR.** Running economy from a muscle energetics perspective. *Front Physiol* 8: 433, 2017. doi:10.3389/fphys.2017.00433.
2. **Russ DW, Elliott MA, Vandenborne K, Walter GA, Binder-Macleod SA.** Metabolic costs of isometric force generation and maintenance of human skeletal muscle. *Am J Physiol Endocrinol Physiol* 282: E448–E457, 2002. doi:10.1152/ajpendo.00285.2001.
3. **Curtin NA, Woledge RC, West TG, Goodwin D, Piercy RJ, Wilson AM.** Energy turnover in mammalian skeletal muscle in contractions mimicking locomotion: effects of stimulus pattern on work, impulse and energetic cost and efficiency. *J Exp Biol* 222: jeb203877, 2019. doi:10.1242/jeb.203877.
4. **Barclay CJ.** Energetics of contraction. In: *Comprehensive Physiology*. Wiley, 2015, p. 961–995.
5. **Stainsby WN, Lambert CR.** Determinants of oxygen uptake in skeletal muscle. *Exerc Sport Sci Rev* 7: 125–152, 1979. doi:10.1249/00003677-197900070-00006.
6. **Woledge RC, Curtin NA, Homsher E.** Energetic aspects of muscle contraction. *Monogr Physiol Soc* 41: 1–357, 1985.
7. **Holt NC, Roberts TJ, Askew GN.** The energetic benefits of tendon springs in running: is the reduction of muscle work important? *J Exp Biol* 217: 4365–4371, 2014. doi:10.1242/jeb.112813.
8. **Joumaa V, Herzog W.** Energy cost of force production is reduced after active stretch in skinned muscle fibres. *J Biomech* 46: 1135–1139, 2013. doi:10.1016/j.jbiomech.2013.01.008.
9. **Cooper AN, McDermott WJ, Martin JC, Dulaney SO, Carrier DR.** Great power comes at a high (locomotor) cost: the role of muscle fascicle length in the power versus economy performance trade-off. *J Exp Biol* 224: jeb236679, 2021. doi:10.1242/jeb.236679.
10. **Gordon AM, Huxley AF, Julian FJ.** The variation in isometric tension with sarcomere length in vertebrate muscle fibres. *J Physiol* 184: 170–192, 1966. doi:10.1113/jphysiol.1966.sp007909.
11. **Barclay CJ.** Energy demand and supply in human skeletal muscle. *J Muscle Res Cell Motil* 38: 143–155, 2017. doi:10.1007/s10974-017-9467-7.
12. **Bohm S, Mersmann F, Santuz A, Arampatzis A.** The force-length-velocity potential of the human soleus muscle is related to the energetic cost of running. *Proc Biol Sci* 286: 20192560, 2019. doi:10.1098/rspb.2019.2560.
13. **Williams CD, Salcedo MK, Irving TC, Regnier M, Daniel TL.** The length-tension curve in muscle depends on lattice spacing. *Proc Biol Sci* 280: 20130697, 2013. doi:10.1098/rspb.2013.0697.
14. **Ichinose Y, Kawakami Y, Ito M, Fukunaga T.** Estimation of active force-length characteristics of human vastus lateralis muscle. *Acta Anat (Basel)* 159: 78–83, 1997. doi:10.1159/000147969.
15. **Holt NC, Azizi E.** What drives activation-dependent shifts in the force–length curve? *Biol Lett* 10: 20140651, 2014. doi:10.1098/rsbl.2014.0651.
16. **Hilber K, Sun YB, Irving M.** Effects of sarcomere length and temperature on the rate of ATP utilisation by rabbit psoas muscle fibres. *J Physiol* 531: 771–780, 2001. doi:10.1111/j.1469-7793.2001.0771h.x.
17. **Stephenson DG, Stewart AW, Wilson GJ.** Dissociation of force from myofibrillar MgATPase and stiffness at short sarcomere lengths in rat and toad skeletal muscle. *J Physiol* 410: 351–366, 1989. doi:10.1113/jphysiol.1989.sp017537.
18. **Beck ON, Trejo LH, Schroeder JN, Franz JR, Sawicki GS.** Shorter muscle fascicle operating lengths increase the metabolic cost of cyclic force production. *J Appl Physiol* (1985) 133: 524–533, 2022. doi:10.1152/jappphysiol.00720.2021.
19. **David Williams C, Regnier M, Daniel TL.** Axial and radial forces of cross-bridges depend on lattice spacing. *PLoS Comput Biol* 6: e1001018, 2010. doi:10.1371/JOURNAL.PCBI.1001018.
20. **MacIntosh BR, MacNaughton MB.** The length dependence of muscle active force: considerations for parallel elastic properties. *J Appl Physiol* (1985) 98: 1666–1673, 2005. doi:10.1152/jappphysiol.01045.2004.
21. **Stainsby WN, Barclay JK.** Relation of load, rest length, work, and shortening to oxygen uptake by in situ dog semitendinosus. *Am J Physiol* 221: 1238–1242, 1971. doi:10.1152/ajplegacy.1971.221.5.1238.
22. **Ortega JO, Lindstedt SL, Nelson FE, Jubrias SA, Kushmerick MJ, Conley KE.** Muscle force, work and cost: a novel technique to revisit the Fenn effect. *J Exp Biol* 218: 2075–2082, 2015. doi:10.1242/jeb.114512.
23. **Fenn WO.** The relation between the work performed and the energy liberated in muscular contraction. *J Physiol* 58: 373–395, 1924. doi:10.1113/JPHYSIOL.1924.SP002141.
24. **Blazevich AJ, Fletcher JR.** More than energy cost: multiple benefits of the long Achilles tendon in human walking and running. *Biol Rev Camb Philos Soc* 98: 2210–2225, 2023. doi:10.1111/brv.13002.
25. **Fletcher JR, MacIntosh BR.** Achilles tendon strain energy in distance running: consider the muscle energy cost. *J Appl Physiol* (1985) 118: 193–199, 2015. doi:10.1152/jappphysiol.00732.2014.
26. **Kram R, Taylor CR.** Energetics of running: a new perspective. *Nature* 346: 265–267, 1990. doi:10.1038/346265a0.
27. **Fletcher JR, Groves EM, Pfister TR, MacIntosh BR.** Can muscle shortening alone, explain the energy cost of muscle contraction in vivo? *Eur J Appl Physiol* 113: 2313–2322, 2013. doi:10.1007/s00421-013-2665-0.
28. **Gill PK, Kipp S, Beck ON, Kram R.** It is time to abandon single-value oxygen uptake energy equivalents. *J Appl Physiol* (1985) 134: 887–890, 2023. doi:10.1152/JAPPLPHYSIOL.00353.2022.
29. **Beck ON, Gosyne J, Franz JR, Sawicki GS.** Cyclically producing the same average muscle-tendon force with a smaller duty increases metabolic rate. *Proc Biol Sci* 287: 20200431, 2020. doi:10.1098/rspb.2020.0431.
30. **Lemaire KK, Baan GC, Jaspers RT, van Soest AJK.** Comparison of the validity of Hill and Huxley muscle tendon complex models using experimental data obtained from rat m. soleus in situ. *J Exp Biol* 219: 977–987, 2016 [Erratum in *J Exp Biol* 219: 2228, 2016]. doi:10.1242/jeb.144394.
31. **MacDougall KB, Kristensen AM, MacIntosh BR.** Additional in-series compliance does not affect the length dependence of activation in rat medial gastrocnemius. *Exp Physiol* 105: 1907–1917, 2020. doi:10.1113/EP088940.
32. **Hamaoka T, McCully KK, Quaresima V, Yamamoto K, Chance B.** Near-infrared spectroscopy/imaging for monitoring muscle oxygenation and oxidative metabolism in healthy and diseased humans. *J Biomed Opt* 12: 062105, 2007. doi:10.1117/1.2805437.
33. **Muthalib M, Millet GY, Quaresima V, Nosaka K.** Reliability of near-infrared spectroscopy for measuring biceps brachii oxygenation during sustained and repeated isometric contractions. *J Biomed Opt* 15: 017008, 2010. doi:10.1117/1.3309746.
34. **Van Beekvelt MC, Colier WN, Wevers RA, Van Engelen BG.** Performance of near-infrared spectroscopy in measuring local O(2) consumption and blood flow in skeletal muscle. *J Appl Physiol* (1985) 90: 511–519, 2001. doi:10.1152/jappphysiol.2001.90.2.511.
35. **Dennis JJ, Wiggins CC, Smith JR, Isautier JMJ, Johnson BD, Joyner MJ, Cross TJ.** Measurement of muscle blood flow and O2 uptake via near-infrared spectroscopy using a novel occlusion protocol. *Sci Rep* 11: 918, 2021. doi:10.1038/s41598-020-79741-w.
36. **Knuth ND, Chartier GL, Dietz GE, Landers-Ramos RQ.** Comparison of near-infrared spectroscopy measured muscle oxygen consumption with whole body oxygen consumption. *Med Sci Sports Exerc* 55: 230–230, 2023. doi:10.1249/01.MSS.0000981856.70081.46.
37. **Fritz CO, Morris PE, Richler JJ.** Effect size estimates: current use, calculations, and interpretation. *J Exp Psychol Gen* 141: 2–18, 2012 [Erratum in *J Exp Psychol Gen* 141: 30, 2012]. doi:10.1037/a0024338.
38. **Aydin O, Yassikaya MY.** Validity and reliability analysis of the PlotDigitizer Software Program for data extraction from single-case graphs. *Perspect Behav Sci* 45: 239–257, 2022. doi:10.1007/S40614-021-00284-0/FIGURES/3.
39. **Hermens HJ, Freriks B, Disselhorst-Klug C, Rau G.** Development of recommendations for SEMG sensors and sensor placement procedures. *J Electromyogr Kinesiol* 10: 361–374, 2000. doi:10.1016/S1050-6411(00)00027-4.
40. **Stegeman DF, Hermens HJ.** *Standards for Surface Electromyography: The European Project “Surface EMG for Non-Invasive Assessment of Muscles (SENIAM)*. Roessingh Research and Development, 2007, vol. 10, p. 8–12.

41. **Fuglevand AJ, Winter DA, Patla AE.** Models of recruitment and rate coding organization in motor-unit pools. *J Neurophysiol* 70: 2470–2488, 1993. doi:10.1152/jn.1993.70.6.2470.
42. **Hullfish TJ, Baxter JR.** A simple instrumented insole algorithm to estimate plantar flexion moments. *Gait Posture* 79: 92–95, 2020. doi:10.1016/j.gaitpost.2020.04.016.
43. **Fukunaga T, Roy RR, Shellock FG, Hodgson JA, Day MK, Lee PL, Kwong-Fu H, Edgerton VR.** Physiological cross-sectional area of human leg muscles based on magnetic resonance imaging. *J Orthop Res* 10: 928–934, 1992. doi:10.1002/jor.1100100623.
44. **Ryan TE, Erickson ML, Brizendine JT, Young HJ, McCully KK.** Noninvasive evaluation of skeletal muscle mitochondrial capacity with near-infrared spectroscopy: correcting for blood volume changes. *J Appl Physiol (1985)* 113: 175–183, 2012. doi:10.1152/jappphysiol.00319.2012.
45. **Fletcher JR, MacIntosh BR.** Estimates of Achilles tendon moment arm length at different ankle joint angles: effect of passive moment. *J Appl Biomech* 34: 220–225, 2018. doi:10.1123/jab.2016-0263.
46. **Edgerton VR, Smith JL, Simpson DR.** Muscle fibre type populations of human leg muscles. *Histochem J* 7: 259–266, 1975. doi:10.1007/BF01003594.
47. **Chow JW, Darling WG.** The maximum shortening velocity of muscle should be scaled with activation. *J Appl Physiol (1985)* 86: 1025–1031, 1999. doi:10.1152/jappl.1999.86.3.1025.
48. **Barclay CJ.** Energetics of contraction. *Compr Physiol* 5: 961–995, 2015. doi:10.1002/cphy.c140038.
49. **Umberger BR, Gerritsen KG, Martin PE.** A model of human muscle energy expenditure. *Comput Methods Biomech Biomed Engin* 6: 99–111, 2003 [Erratum in *Comput Methods Biomech Biomed Engin* 9: 342, 2006]. doi:10.1080/1025584031000091678.
50. **Bhargava LJ, Pandy MG, Anderson FC.** A phenomenological model for estimating metabolic energy consumption in muscle contraction. *J Biomech* 37: 81–88, 2004. doi:10.1016/S0021-9290(03)00239-2.
51. **Fletcher JR, MacIntosh BR.** Theoretical considerations for muscle-energy savings during distance running. *J Biomech* 73: 73–79, 2018. doi:10.1016/j.jbiomech.2018.03.023.
52. **Shimizu S, Chiarotti F, Ferrari M, Kagaya A, Quaresima V, Homma S, Azuma K.** Calf and shin muscle oxygenation patterns and femoral artery blood flow during dynamic plantar flexion exercise in humans. *Eur J Appl Physiol* 84: 387–394, 2001. doi:10.1007/s004210100390.
53. **Homsher E, Mommaerts WF, Ricchiuti NV, Wallner A.** Activation heat, activation metabolism and tension-related heat in frog semitendinosus muscles. *J Physiol* 220: 601–625, 1972. doi:10.1113/jphysiol.1972.sp009725.
54. **Barclay CJ.** Mechanical efficiency and fatigue of fast and slow muscles of the mouse. *J Physiol* 497: 781–794, 1996. doi:10.1113/jphysiol.1996.sp021809.
55. **Smith NP, Barclay CJ, Loisel DS.** The efficiency of muscle contraction. *Prog Biophys Mol Biol* 88: 1–58, 2005. doi:10.1016/j.pbiomolbio.2003.11.014.
56. **Rack PM, Westbury DR.** The effects of length and stimulus rate on tension in the isometric cat soleus muscle. *J Physiol* 204: 443–460, 1969. doi:10.1113/jphysiol.1969.sp008923.
57. **Stainsby WN, Barclay JK.** Effect of infusions of osmotically active substances on muscle blood flow and systemic blood pressure. *Circ Res* 28: 33–8, 1971.